HYPERBOLICITY OF AUGMENTED LINKS IN THE THICKENED TORUS

ALICE KWON AND YING HONG THAM

Abstract. For a hyperbolic link K in the thickened torus, We show there is a decomposition of the complement of a link L, obtained from augmenting K, into torihedra. We further decompose the torihedra into angled pyramids and finally angled tetrahedra. These fit into an angled structure on a triangulation of the link complement, and thus by [5], this shows that L is hyperbolic.

1. Introduction

Given a twist reduced diagram of a link K, *augmenting* is a process in which an unknotted circle component (augmentation) is added to one or more twist regions (a single crossing or a string of bigons) of K. The added circle component allows us to remove full twists at the twist region of K. If the twist region has an odd number of crossings then all but one crossing is removed, whereas if the twist region has an even number of crossings then all are removed. The newly obtained link is called an *augmented link* and the newly obtained diagram is called an *augmented link diagram*. See Figure 2.

Adams showed in [1] that given a hyperbolic alternating link K in S^3 the link L obtained by augmenting K is hyperbolic. In this paper we investigate if this statement holds for links in the thickened torus i.e. if L is a link obtained from augmenting a hyperbolic alternating link K in the thickened torus. We define augmenting similarly for links in the thickened torus with their associated link diagram on $\mathbb{T}^2 \times \{0\}$.

Menasco [7] showed there are decompositions of the complements of alternating links in S^3 into two polyhedra, a top polyhedron and a bottom polyhedron. For alternating links K in the thickened torus, Champanerkar, Kofman and Purcell [3] showed that there is a decomposition of the complement of K into objects called torihedra, which we think of as counterparts to Menasco's decomposition of links in S^3 into polyhedra, for links in the thickened torus. Just like Menasco's decomposition, one obtains a top and a bottom torihedron. In Section 2 we show that for augmented links in the thickened torus one can also obtain a decomposition of the complement into a top and bottom torihedron. In Section 3, we prove that many augmented alternating links in the thickened torus are hyperbolic. In the Appendix, we provide an alternative proof to hyperbolicity of these links via circle patterns, which one could use to obtain lower bounds for volume.

2. Augmented Links

Champanerkar, Kofman and Purcell have studied alternating links in the thickened torus [3]. They define a link in the thickened torus as a quotient of a biperiodic alternating link as follows,

Definition 2.1. A *biperiodic alternating link* $\mathcal{L}$ is an infinite link which has a projection onto $\mathbb{R}^2$ which is invariant under an action of a two dimensional lattice Λ by translations,

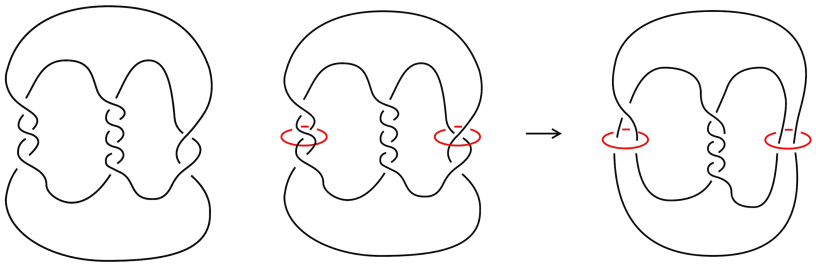

(a) (b)

FIGURE 1. The left shows a pretzel knot before augmentation and the right shows after augmentation

such that $L = \mathcal{L}/\Lambda$ is an alternating link in $\mathbb{T}^2 \times I$, where $I = (-1, 1)$, with the projection on $\mathbb{T}^2 \times \{0\}$. We call L a link diagram in $\mathbb{T}^2 \times I$.

Remark 2.2. Since $\mathbb{T}^2 \times I \cong \mathrm{S}^3 - H$, where H is a Hopf link. The complement $\mathbb{T}^2 \times I - L = \mathrm{S}^3 - (L \cup H)$.

Champanerkar, Kofman and Purcell [3] extended the definition of prime links in S^3 for links in $\mathbb{T}^2 \times I$ called weakly prime.

Definition 2.3. A diagram of a link L is *weakly prime* if whenever a disk is embedded in the diagram surface meets the diagram transversely in exactly two edges, then the disk contains a simple edge of the diagram and no crossings.

Definition 2.4. A *twist region* in a link diagram $L = \mathcal{L}/\Lambda$ in $\mathbb{T}^2 \times I$, is the quotient of a twist region in the biperiodic link $\mathcal{L}$. universal cover of $\mathbb{T}^2 \times I$ is called a . A biperiodic link $\mathcal{L}$ is called *twist-reduced* if for any simple closed curve on the plane that intersects $\mathcal{L}$ transversely in four points, with two points adjacent to one crossing and the other two points adjacent to another crossing, the simple closed curve bounds a subdiagram consisting of a (possibly empty) collection of bigons strung end to end between these crossings. We say L is *twist-reduced* if it is the quotient of a twist-reduced biperiodic link.

Now we can define augmentation for a link in $\mathbb{T}^2 \times I$ the same way we define augmentation for links in S^3. For a link in $\mathbb{T}^2 \times I$, the crossing circles are added to the diagram projected onto $\mathbb{T}^2 \times \{0\}$. Let L be a twist reduced diagram in $\mathbb{T}^2 \times I$, we define *augmenting* as a process in which an unknotted circle component is added to one or more twist regions of L. See Figure 2

2.1. **Torihedral Decomposition of Augmented Alternating Links in Thickened Torus.** We present a method of decomposing an augmented link in the thickened torus into objects called "torihedra" as defined below. The idea is to combine methods of Menasco [7] and the use of crossing edges between each crossing of our link and Lackenby's "cut-slice-flatten" method [6] on the augmentation sites.

Definition 2.5. [3] A *torihedron* $\mathcal{T}$ is a cone on the torus, i.e. $\mathbb{T}^2 \times [0, 1]/(\mathbb{T}^2 \times \{1\})$, with a cellular graph $G = G(\mathcal{T})$ on $\mathbb{T}^2 \times \{0\}$. An *ideal torihedron* is a torihedron with the vertices of G and the vertex $\mathbb{T}^2 \times \{1\}$ removed. Hence, an ideal torihedron is homeomorphic to $\mathbb{T}^2 \times [0, 1)$ with a finite set of points (ideal vertices) removed from $\mathbb{T}^2 \times \{0\}$. We refer to the vertex $\mathbb{T}^2 \times \{1\}$ as the cone point.

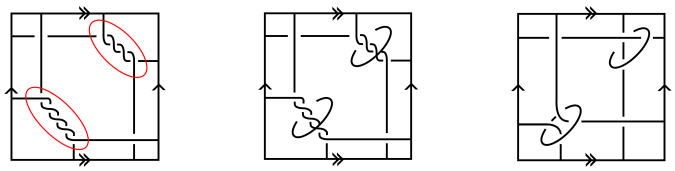

FIGURE 2. A: The top right has an odd number of twists while the bottom left has an even number of twists. B: The picture of the link on the right after augmentation twist regions circled in red. C: The link with the twists removed.

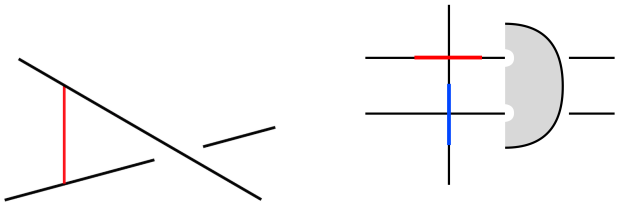

FIGURE 3. Left: The black strands are part of the link and the red strand is the crossing edge. Right: The blue and red edges represent the split crossing edges and the shaded half disk is bounded by the crossing circle

For visualization purposes, we typically draw the graph $G(\mathcal{T})$ of a torihedron from the perspective of the cone point $\mathbb{T}^2 \times \{1\}$.

If the faces of $G(\mathcal{T})$ are disks, then $\mathcal{T}$ can be decomposed into a union of pyramids, obtained by coning each face to the cone point of $\mathcal{T}$. This also gives a decomposition of the corresponding ideal torihedron into ideal pyramids. We call these the *pyramidal decompositions* of $\mathcal{T}$ and its ideal version.

Proposition 2.6. *Let L be an augmented link in $\mathbb{T}^2 \times I$. There is a decomposition of the complement, $(\mathbb{T}^2 \times I) - L$ into two ideal torihedra.*

Proof. We will begin by assuming that there are no half twists. Arrange the link diagram of L in the following way: first place the added circle components perpendicular to the projection plane, $\mathbb{T}^2 \times \{0\}$ leaving the remaining part of the link parallel to the projection plane. We now place a crossing edge on each crossing of the link so that for each crossing edge, one end of the edge lies on a bottom strand while the other end lies on a top strand as in Figure 3 left.

We view the link from the point at infinity from the top. We will push the top strand to the bottom strand, splitting the crossing edge into two identical edges as in Figure 3 right. We push the link components to infinity and stretch the crossing edge so that we have flattened the link onto $\mathbb{T}^2 \times \{0\}$ except for the crossing circles which will remain perpendicular to the projection plane.

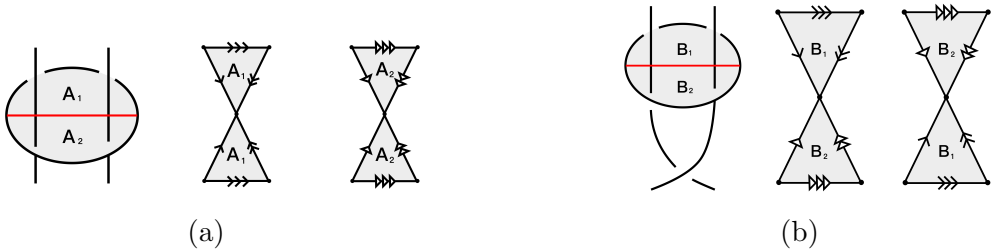

(a) (b)

FIGURE 4. (a) Gluing of bow-ties without half-twists (b) Gluing with half-twists

Now place a disk on each crossing circle, so that the disk is bounded by the crossing circle. We can then cut $\mathbb{T}^2 \times I$ along $\mathbb{T}^2 \times \{0\}$ and focus on the top half, $\mathbb{T}^2 \times [0, 1)$. We will follow the same method on the bottom half to obtain the second identical torihedron. The disk we place on each crossing circle is now cut in half. This half disk is now bounded by the projection plane and the semi-cricle arc of the crossing circle. We push down on the crossing circle and split the disk into two identical disks. We then push the arc of each crossing circle to infinity, collapsing them to ideal vertices. We obtain two triangular faces which represent the disk which look like a bow-tie as in Figure 4.

We repeat the steps for the bottom half of $\mathbb{T}^2 \times I$, $\mathbb{T}^2 \times (-1, 0]$. Then we get two torihedra. The graph of each will come from crossing edges and edges of the disk. Now, if there are half twists we will decompose the complement of the link the same way as if there are no half twists and we will identify the two bow-ties as in Figure 4. Finally, we obtain the complement of the link by gluing the two torihedra with the gluing information given by identifying crossing edges and triangles of the bow-tie. We glue the faces of the torihedra which do not correspond to a bow-tie with a $2\pi/n$ twist where n is the number of sides of each face as in Figure 8 clockwise or counterclockwise.

For future reference, we will denote the graph for the top and bottom torihedra by $\Gamma_T(L)$ and $\Gamma_B(L)$, respectively, where both graphs are viewed from the cone point of the top torihedron $\mathbb{T}^2 \times \{1\}$. Note that if $L = K$ is the non-augmented link, $\Gamma_T(L)$ is simply the link projection K, and in fact $\Gamma_T(K) = \Gamma_B(K)$.

□

The Figures 5 to 8 is an example which decomposes the link (C) of Figure 2.

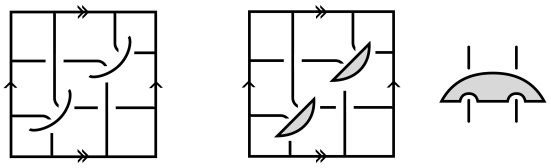

FIGURE 5. Each crossing circle bounds a twice-punctured disk

Definition 2.7. An *angled torihedron* $(\mathcal{T}, \theta^*_\bullet)$ is a torihedron $\mathcal{T}$ with an assignment $\theta^*_e \in [0, \pi]$ such that for each vertex $v \in G(\mathcal{T})$, $\sum_{e \ni v} \theta^*_e = (\deg(v) - 2)\pi$. We also denote $\theta_e = \pi - \theta^*_e$, so $\sum_{e \ni v} \theta_e = 2\pi$; we refer to θ_e as the exterior angle and θ_e as the interior angle.

We say $(\mathcal{T}, \theta^*_\bullet)$ is *degenerate* if $\theta^*_e = 0$ for some edge; we say it is *non-degenerate* otherwise.

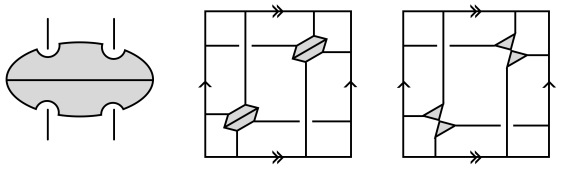

FIGURE 6. We split the disk and collapse the arc of each crossing circle to ideal vertices

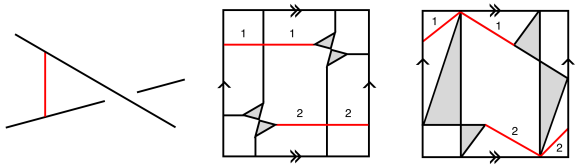

FIGURE 7. Left: The crossing arc is the edge in red. Middle: Picture of splitting the crossing edge. Right: The link component is pushed off to infinity.

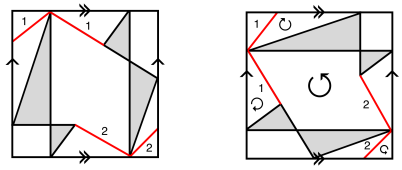

FIGURE 8. Left: The top torihedron. Right: The bottom torihdron with rotation for face gluing.

One may ask for the pyramidal decomposition of a torihedron to "respect" angles. The following definitions, in particular an "angle splitting", make sense of this.

Definition 2.8. An *angled ideal tetrahedron* is an ideal tetrahedron with an assignment of a dihedral angle to each edge, such that

- each dihedral angle is in $[0, \pi]$;
- for each tetrahedron, opposite edges have equal dihedral angles;
- the three distinct angles sum to π.

We say a angled ideal tetrahedron is *degenerate* if one dihedral angle is 0; we say it is *non-degenerate* otherwise.

Definition 2.9. A *base-angled ideal pyramid* is a pyramid whose base is an n-gon, $n \geq 3$, and each boundary edge e_i of the base face is assigned a dihedral angle $\alpha_i \geq 0$ such that the sum is $\sum \alpha_i = 2\pi$. The vertical edge e_i' that meets e_i and e_{i+1} is automatically assigned the dihedral angle $\pi - \alpha_i - \alpha_{i+1}$.

We say a base-angled ideal pyramid is *degenerate* if $\alpha_i = 0$ for some i; we say it is *non-degenerate* otherwise.

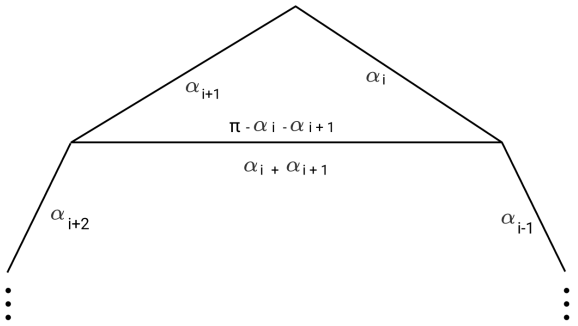

FIGURE 9. Angle-splitting on a polygonal face of the graph

Clearly, the dihedral angles of an ideal hyperbolic pyramid make it a base-angled ideal pyramid (with $\alpha_i = \varphi_{e_i}$); it is not hard to see that the converse is true: simply consider a circumsribed polygon such that the side e_i subtends an angle of $2\alpha_i$ at the center, and take the ideal hyperbolic pyramid over it in upper-half space. Also, an angled ideal tetrahedron is simply a base-angled ideal pyramid with base a triangle, and with no preferred face.

Definition 2.10. An *angle splitting* of an angled torihedron $(\mathcal{T}, \theta^*_\bullet)$ is a splitting of $\theta^*_e = \varphi_{\vec{e}} + \varphi_{\overleftarrow{e}}$ for each edge e, such that for each face f, $\sum_{\vec{e} \in \partial f} \varphi^*_{\vec{e}} = \pi$.

Equivalently, an angle splitting is a decomposition of $\mathcal{T}$ into base-angled pyramids, one for each face of $G(\mathcal{T})$, such that for each boundary edge e of $\mathcal{T}$, the dihedral angles from the two adjacent pyramids add to θ^*_e.

Remark 2.11. These θ's are related to the θ's in [2], and the φ's are related to their "coherent angle system".

Lemma 2.12. *Let P_n be a base-angled ideal pyramid, and suppose we are given a decomposition of the base face into triangles by adding new edges. One gets an obvious corresponding triangulation of P_n, where a new face is added for each new edge. Then there is an assignment of a dihedral angle to each edge of each ideal tetrahedron in this triangulation such that*

- *each tetrahedron is an angled ideal tetrahedron;*
- *the sum of dihedral angles around each new edge is π;*
- *the dihedral angles of the edges of the original base face are the same as before.*

Proof. Induct on n; there is nothing to prove for the base case $n = 3$.

The proof is essentially given in Figure 9.

Suppose the edges are labeled e_i, which goes between vertices v_i and v_{i+1}, and suppose e_i is assigned dihedral angle α_i. Let e' be a new edge addeed to the base face of P_n such that it separates the base face into a triangle and an $(n-1)$-gon; suppose the sides of the triangle are e_i, e_{i+1}, and e'. The new face corresponding to e' separates P_n into an ideal tetrahedron T and an ideal pyramid P_{n-1}. We assign the dihedral angle of $\pi - \alpha_i - \alpha_{i+1}$ to e' in T, and assign $\alpha_i + \alpha_{i+1}$ to e' in P_{n-1}. Clearly the sum of dihedral angles condition is satisfied in T and P_{n-1}. It remains to check that the dihedral angles assigned to the vertical (non-base) edges are correct. For the vertical edge associated to v_j for $j \neq i, i+2$, there is nothing to check; for $j = i$, the dihedral angles are $\pi - \alpha_i - (\pi - \alpha_i - \alpha_{i-1})$ in T and $\pi - \alpha_{i-1} - (\alpha_i + \alpha_{i+1})$ in P_{n-1}, which sum to $\pi - \alpha_i - \alpha_{i+1}$; it is similar for $j = i + 2$.

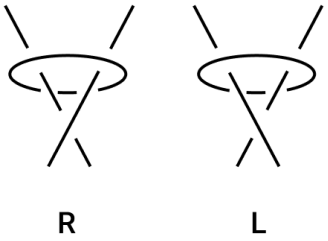

FIGURE 10. R: right augmentation, L: left augmentation

□

3. Hyperbolicity of Augmented Links

Thurston introduced a method for finding the unique hyperbolic metric for a given 3-manifold M with boundary consisting of tori [8]. The idea was to triangulate the interior of M into ideal tetrahedra and give those tetrahedra hyperbolic shapes (called shape parameters) that glue up coherently in M. The shape parameter of a tetrahedron is described by the cross-ratio of its four vertices on the sphere at infinity. Thurston had written down a system of gluing equations with shape parameters whose solutions correspond to the complete hyperbolic metric on the interior of M. Casson and Rivin separated gluing equations into a linear and non-linear part [5]. Angle structures is the linear part of Thurston's gluing equations, and what we will use to attain hyperbolicity of complements of augmented links in the thickened torus.

Definition 3.1. Let M be an orientable 3-manifold with boundary consisting of tori. An angle structure on an ideal triangulation τ of M is an assignment of a dihedral angle to each edge of each tetrahedron, such that

- each tetrahedron is a non-degenerate angled ideal tetrahedron,
- around each edge of τ, the dihedral angles sum to 2π.

Theorem 3.2. [5] *Let M be a 3-manifold admitting an angle structure. Then M is hyperbolic.*

For a hyperbolic link K in $\mathbb{T}^2 \times I$, we show that the resulting link obtained from augmenting K is hyperbolic. The idea is to start with a graph from the torihedral decomposition of the link K which will give us a graph on each torihedron with an angle assignment of $\pi/2$ for edge [3], the angled torihedra can be further decomposed into base-angled pyramids. By Proposition 2.6, there is a torihedral decomposition of the complement of the augmented link L. Using those angles, we then assign angles to edges of these torihedra and decompose them into base-angled pyramids. These pyramids can be further decomposed into tetrahedra, thus obtaining an angle structure on a triangulation. In the Appendix, we show that this triangulation also has an angle structure that satisfies Thurston's gluing equations.

Definition 3.3. We say an augmentation is *right-augmented* if, when both strands are (locally) oriented such that they cross the augmentation disk in the same direction, the crossing is a positive right-handed half-twist. See Figure 10. We say an augmentation is *left-augmented* if it is not right-augmented.

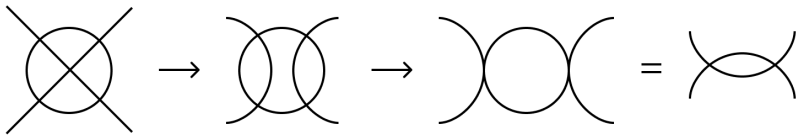

FIGURE 11. Resolving internal vertex; eliminating bigons via "crushing"

We can recover L from the link diagram of K together with labels at vertices indicating left- or right-augmentation.

Lemma 3.4. *Let G be a 4-valent graph on $\mathbb{T}^2$ with no bigons or self-loops. Then for any subset $F' \subseteq F$ of faces,*

$$2\chi(F') \leq |E'|$$

where $E' = \cup_{f \in F'} \partial f$ is the set of edges that meets some face of F', and $\chi(F') = \sum_{f \in F'} \chi(f)$ is the sum of the Euler characteristics of faces in F'.

Proof. We induct on $\chi(F')$ (over all possible such graphs G); for $F' = \emptyset$, there is nothing to prove.

Call a vertex or edge *interior* if it does not meet $F'' = F \backslash F'$. Suppose there is an interior vertex v. Make the modification as in Figure 11 (later we will choose which way to "resolve" the vertex). This decreases $\chi(F')$ by one and $|E'|$ by 2. However, this process may produce bigons; if it does, repeatedly eliminate bigons by either (1) performing the modification as in Figure 11 if the two vertices of the bigon are distinct, or (2) remove the bigon completely if the two vertices of the bigon are the same. Each of these steps also decreases $\chi(F')$ by one and $|E'|$ by 2 (note in the second case, after removing the bigon, the operation merges two distinct faces or joins a face to itself; this adds an S^1, thus does not change the (total) euler characteristic of the two faces or the one face).

We must check that this process terminates with a graph which satisfies the hypotheses set out in the lemma. It is clear that 4-valency is maintained at each step, and there will not be any bigons at the end. We need to ensure that eliminating bigons does not create self-loop edges. Here we specify how to choose which way to resolve the internal vertex v. If among the four faces touching v, one of them has greater than three sides (Case 1), then resolve v so that this face is not merged; if all four faces are triangles (Case 2), simply resolve in an arbitrary manner. After the modification of the internal vertex, at most two bigons are created; eliminate those two bigons. Now we find that all bigons will be connected end-to-end (i.e. forming a single twist region) - this is because in Case 1, only one bigon was present after smoothing v, which would result in at most two bigons that would be connected; and if we were in Case 2, we find that the face between those eliminated bigons (coming from merging the two triangles across v) will become a bigon too, thus connecting the potential bigons on either ends.

Therefore, one can eliminate bigons in an order so that they belong in one twist region; in particular, the (not necessarily distinct) faces on either side are not bigons, so eliminating the bigon does not produce a self-loop edge.

Now suppose G has no interior vertices. We perform some reductions. We remove all f from F' that have non-positive Euler characteristic, as doing so will not decrease $\chi(F')$ and will not increase $|E'|$. Now consider some $f \in F'$. If it has at least two boundary (i.e.

non-interior) edges, we can remove f from F', which decreases $\chi(F')$ by 1 and $|E'|$ by at least 2. Thus we remove all such f.

Now suppose $f \in F'$ has three contiguous interior edges e_1, e_2, e_3. (e.g. if f has at least four sides). Let v_1, v_2 be the vertices between these three interior edges. Since v_1 is not interior, the face across v_1 from f is not in F'; likewise with v_2. But this shows that the face across e_2 from f has two boundary edges, contradicting our reduction.

Thus, we now have a graph whose faces are triangles, and each face has exactly one boundary edge. Now the problem is solved with a simple counting argument: each f corresponds to one boundary edge and two interior edges, but, since the interior edges are shared by two faces, they should count as half an edge; so

$$|E'| = \sum_{f \in F'} 1 + 1/2 + 1/2 = 2|F'| = 2\chi(F')$$

and we get the desired result. □

The following theorem is quoted from [2] (see also [4])

Theorem 3.5 (Feasible Flow Theorem)**.** *Let (N, X) be a directed graph, with a* lower capacity bound a_x *and* upper capacity bound b_x *for each directed edge $x \in X$, with $-\infty \leq a_x \leq b_x \leq \infty$. A* feasible flow *is a function $\varphi : X \to \mathbb{R}$ such that $\varphi_x \in [a_x, b_x]$ and Kirchhof's current law is satisfied (i.e. flow in = flow out at every vertex).*

A feasible flow exists if and only if, for every proper nonempty subset $N' \subset N$,

$$\sum_{x \in ex(N')} b_x \geq \sum_{x \in in(N')} a_x$$

where $ex(N'), in(N')$ refer to edges leaving, entering N', respectively.

Theorem 3.6. *Let K be a weakly prime, alternating link whose diagram has no bigons. Let L be a link obtained from augmenting K. Then L is hyperbolic.*

Proof. By [3, Theorem 7.5], (as discussed in Proposition 2.6,) $\mathbb{T}^2 \times I - K$ can be decomposed into two torihedra $\mathcal{T}_T$ and $\mathcal{T}_B$, whose graphs are $\Gamma_T(K), \Gamma_B(K)$ respectively; viewed from the top cone point $\mathbb{T}^2 \times \{1\}$, they are both the same as the projection graph of K. We make them non-degenerate angled torihedra by assigning $\theta^* = \pi/2$ for all edges.

We obtain an angle-splitting by applying the Feasible Flow theorem (Theorem 3.5) as follows: Consider the directed graph whose vertex set is $E \cup F \cup \{*\}$, where E, F are the set of edges, faces of $\Gamma_T(K)$ respectively, and there is a directed edge

- $* \to f$ for each face $f \in F$, with capacity interval $[\pi, \infty)$,
- $f \to e$ for each edge $e \in \partial f$, with capacity interval $[\varepsilon, \infty)$ for some $\varepsilon > 0$ to be set later,
- $e \to *$ for each edge e, with capacity interval $(-\infty, \pi/2]$.

By Lemma 3.4, $2|F'| = 2\chi(F') \leq |E'|$, and taking $\varepsilon < \pi/|\text{max face size}|$, the feasible flow condition is satisfied, so a feasible flow exists. Since $2|F| = |E|$, the capacity interval restrictions on the flow at $*$ is sharp, so out-edges at $*$ have flow π and in-edges at $*$ have flow $\pi/2$. Then the flow $f \to e$ gives us $\varphi_{\vec{e}}$, where f is the face to the left of $\vec{e}$. (We adapted this argument from [2]).

By Proposition 2.6, $\mathbb{T}^2 \times I - L$ can be obtained by gluing two torihedra $\mathcal{T}_T(L), \mathcal{T}_B(L)$ with graphs $\Gamma_T(L), \Gamma_B(L)$. We make them degenerate angled torihedra by assigning θ^*'s to edges of the bow-ties as in Figure 12, and assign $\pi/2$ to all other edges. It is easy to check that

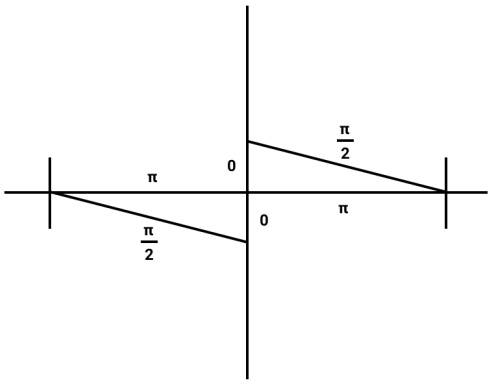

FIGURE 12. Angle assignments on a bow-tie corresponding to an augmentation site

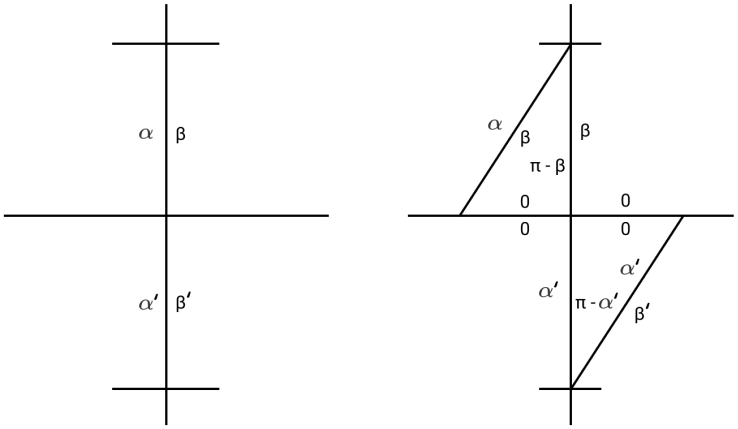

(a) (b)

FIGURE 13. (a) Angles before augmentation (b) Angle splitting for bowtie corresponding to augmentation

upon gluing, each edge has sum of dihedral angles (θ^*) equals 2π. (This holds true even if they were glued assuming some augmentations had no half-twist; see Remark 3.7.)

Furthermore, we can obtain an angle-splitting of $\mathcal{T}_T(L)$ (and similarly $\mathcal{T}_B(L)$) by modifying the angle-splitting for $\mathcal{T}_T(K)$; this is shown in Figure 13.

Now we have a decomposition of the two torihedra into degenerate base-angled pyramids. However, we need the pyramids to be non-degenerate, so we first need to modify the angles and graph on the torihedra to make all θ^* nonzero.

Consider a face f of $\Gamma_T(L)$ that is not in a bow-tie. Suppose the corresponding face $\bar{f}$ of Γ, the projection graph (which is equal to $\Gamma_T(K)$), had vertices $v_1, \ldots, v_n$ in counter-clockwise order. We label the edges of f by $e_{i,0}$, $e_{i,\pi}$, or e_i, depending on whether the θ^* is 0, π, or $\pi/2$ respectively, with i non-decreasing from 1 to n, adjacent edges having the same i if and only if they belong to the same bow-tie. For sake of concreteness, suppose that if a vertex v_i is right-augmented, then the augmentation circle intersects $\bar{f}$ (everything is similar if it

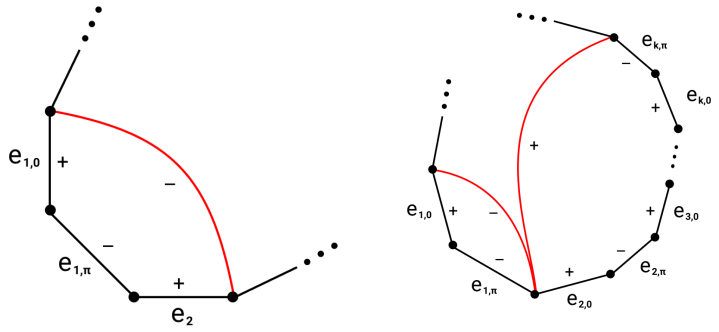

FIGURE 14. Red edge indicates an added edge to the graph to appropriately assign +/- labels which indicate increasing/decreasing angles on the edge respectively.

is left-augmented vertices' circles that intersect $\bar{f}$). In other words, locally, f meets two of the edges of the bow-tie corresponding to a right-augmented vertex v_i (which would be labeled $e_{i,0}, e_{i,\pi}$ in counter-clockwise order), but only meets one of the edges of the bow-tie corresponding to a left-augmented vertex.

Suppose, after cyclically reindexing, $v_1, \dots, v_k$ is a maximally contiguous subsequence of left-augmented vertices of $G(K)$ around the face $\bar{f}$; the edges around f would start $e_{1,0}, e_{1,\pi}, e_{2,0}, e_{2,\pi}, \dots$. We add new edges across f as follows. (See Figure 14; ignore the + and - signs for now.)

First suppose $k = n$; then we do nothing.

Next suppose there is only one such maximal contiguous subsequence. If $k = 1$, we add an edge that goes across $e_{1,0}, e_{1,\pi}, e_2$ (in the sense that the new edge separates the edges of f into two sets, one of them being those three edges; since $n \geq 3$, this edge is new). If $k \geq 2$, we add an edge across $e_{1,0}, e_{1,\pi}$ and another edge across $e_{2,0}, e_{2,\pi}, e_{3,0}, \dots, e_{k,\pi}$ (these two edges do not form a bigon because we've ruled out $k = n$).

Finally, if there are multiple such maximal contiguous subsequences, we just add edges as above for each contiguous subsequence. The only caveat is that if the procedure calls to add a new edge that would form a bigon with the existing edges, we just do not add it.

This way we obtain a new graph $\Gamma_T(L)'$, which defines a new torihedron $\mathcal{T}_T(L)'$. We make $\mathcal{T}_T(L)'$ angled using the angles from $\mathcal{T}_T(L)$ for old edges, and putting π for all new edges.

Now we deform the θ^* based on Figure 14, increasing/decreasing by some small $\varepsilon' > 0$ if the edge is labeled $+/-$. Note some edges may be labeled twice, in which case we perform both increasing/decreasing (e.g. if it is labeled + and −, the θ^* is not changed). It is easy to see that the sum of θ^* around a vertex remains unchanged. Furthermore, all the edges with θ^* originally equal 0, i.e. all $e_{i,0}$'s, now have positive θ^*, (it receives only one label +, because the other face it meets is a bow-tie).

We can directly get an angle-splitting for $\mathcal{T}_T(L)'$ using the angle-splitting for $\mathcal{T}_T(L)$. We reuse the $+/-$ assignments from Figure 14. For $e = e_{i,0}$, we increase $\varphi_{\vec{e}}, \varphi_{\overleftarrow{e}}$ by $\varepsilon'/2$ each; for $e = e_{i,\pi}$, we decrease them by $\varepsilon'/2$ each. For other edges, we increase/decrease $\varphi_{\vec{e}}$ by ε', where $\vec{e}$ is the oriented edge corresponding to the side on which the $+/-$ sign appears in Figure 14; so for example, if an edge e receives both + and −, then one of $\varphi_{\vec{e}}, \varphi_{\overleftarrow{e}}$ increases while the other decreases, thus θ^*_e remains constant.

Now we address $\mathcal{T}_B(L)$. In the gluing of $\mathcal{T}_T(L)$ to $\mathcal{T}_B(L)$, non-bow-tie faces of $\Gamma_T(L)$ are identified with non-bow-tie faces of $\Gamma_B(L)$. Under this identification, we add the same edges to $\Gamma_B(L)$, thus obtaining the new torihedron $\mathcal{T}_B(L)'$ with graph $\Gamma_B(L)'$. We perform the same deformations of θ^*'s (or φ's).

We need to check that upon gluing $\mathcal{T}_T(L)'$ to $\mathcal{T}_B(L)'$, the sum of dihedral angles around each edge is still 2π. This was clearly true before deforming, as the new edges of $\Gamma_T(L)'$ only gets identified with the unique corresponding edge of $\Gamma_B(L)'$, and they are both labeled with $\theta^* = \pi$. To see that the deformation does not change these sums, note that in the identification of faces of $\Gamma_T(L)'$ to $\Gamma_B(L)'$, an edge with $\theta^* = 0$ is identified with an edge with $\theta^* = \pi$, so an increase in the former would be conterbalanced by a decrease in the latter. It is also easy to see this is the case for the other edges. (Once again, a similar argument applies if $\mathcal{T}_(L)'$ and $\mathcal{T}_B(L)'$ are glued assuming some augmentations had no half-twist; see Remark 3.7.)

Finally, for each face of $\Gamma_T(L)'$ that has more than three sides, we arbitrarily decompose it into triangles and apply Lemma 2.12 to obtain a triangulation of $\mathcal{T}_T(L)'$ into non-degenerate angled tetrahedra; perform the corresponding decomposition for faces of $\Gamma_B(L)'$ and obtain a triangulation of $\mathcal{T}_B(L)'$ into non-degenerate angled tetrahedra. Upon gluing, this gives an angle structure on the triangulation of $\mathbb{T}^2 \times I - L$ □

Remark 3.7. If the original link K had some twist regions with at least one bigon, we may consider augmentations L where all such twist regions are augmented, i.e. L may have augmentations without half-twists. Then, as pointed out in proof of Theorem 3.6 above, the proof still works for L, showing that L is also hyperbolic.

4. Appendix

We provide an alternative method via circle patterns to obtain an angle-splitting of the torihedral decomposition in Section 2. This guarantees that the resulting angle structure on the final triangulation also satisfies Thurston's gluing equations. Thus, one can obtian lower bounds on volume from these angles.

Let Γ be a graph on the torus $\mathbb{T}^2$, and let V, E, F be the set of vertices, edges, faces, respectively. Generally we assume that graphs do not have bigon faces nor self-loop edges.

$\vec{E}$ is the set of oriented edges. We may identify an oriented edge $\vec{e}$ with the pair $(f_{\vec{e}}, e)$, where $f_{\vec{e}}$ is the face to the left of $\vec{e}$.

When we use $\overleftarrow{e}$ to refer to an oriented edge, it refers to the oppositely oriented edge to $\vec{e}$. If we construct an expression with both $\vec{e}$ and $\overleftarrow{e}$, it will always be (anti-)symmetrical in the two orientations, and we assume that an arbitrary choice has been made.

Recall that a cirlce pattern for a graph Γ is an arrangement of circles in $\mathbb{T}^2$ such that each circle circumscribes a face of Γ. A circle pattern is determined by the radius of the circle C_f associated to each face, r_f, and the angle that each edge subtends in adjacent faces, $\varphi_{\vec{e}}$. (See Figure 15) Thus determines, and is determined by a point in $\underline{\mathfrak{R}} \times \underline{\mathfrak{Q}}$, where

- $\underline{\mathfrak{R}} := \mathbb{R}_+^F = \{(r_f)_{f\in F} | r_f \in \mathbb{R}_+\}$
- $\underline{\mathfrak{Q}} := \mathbb{R}^{\vec{E}} = \{(\varphi_{\vec{e}})_{\vec{e}\in\vec{E}} | \varphi_{\vec{e}} \in \mathbb{R}\}$

but clearly not every point $c \in \underline{\mathfrak{R}} \times \underline{\mathfrak{Q}}$ determines a circle pattern. This larger space allows us to consider "degenerate" circle patterns, where adjacent circles may be identical or tangent.

On $\underline{\mathfrak{R}} \times \underline{\mathfrak{Q}}$, there are several functions to consider:

- $\Phi_f = 2\sum_{\vec{e}\in\partial f} \varphi_{\vec{e}}$, measuring the cone angle at the center of C_f
- $\theta_e = \pi - \varphi_{\vec{e}} - \varphi_{\overleftarrow{e}}$

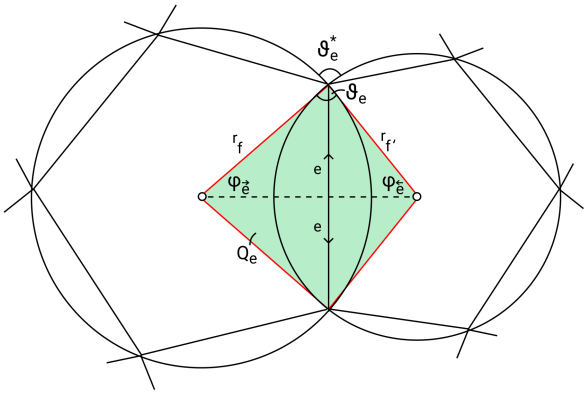

FIGURE 15. Circle pattern in terms of radii r_f and angles $\varphi_{\vec{e}}$

- $l_{\vec{e}} = 2r_{f_{\vec{e}}} \sin \varphi_{\vec{e}}$

These fit together to give maps to the following spaces:

- $\underline{\mathbf{\Phi}} := \mathbb{R}^F = \{(\Phi_f)_{f\in F} | \Phi_f \in \mathbb{R}\}$
- $\underline{\mathbf{\Theta}} := \mathbb{R}^E = \{(\theta_e)_{e\in E} | \theta_e \in \mathbb{R}\}$
- $\underline{\mathfrak{L}} := \mathbb{R}^{\vec{E}} = \{(l_{\vec{e}})_{\vec{e}\in E} | l_{\vec{e}} \in \mathbb{R}\}$

Definition 4.1. Let Γ be a graph on the torus. An *extended circle pattern* on Γ is $c = ((r_f), (\varphi_{\vec{e}})) \in \underline{\mathfrak{R}} \times \underline{\mathfrak{Q}}$ such that $l_{\vec{e}} = l_{\overleftarrow{e}}$ for all edges $e \in E$. We denote by $\underline{\mathfrak{C}}$ the set of extended circle patterns.

$$\begin{array}{ccccc} \underline{\mathfrak{C}} = \{l_{\vec{e}} = l_{\overleftarrow{e}}\} & \xrightarrow{\subset} & \underline{\mathfrak{R}} \times \underline{\mathfrak{Q}} & \xrightarrow{\Theta} & \underline{\mathbf{\Theta}} \\ & & \downarrow{\scriptstyle \Phi} & & \\ & & \underline{\mathbf{\Phi}} & & \end{array}$$

The notion of a circle pattern that is considered in [2] would be restricted to those $c \in \underline{\mathfrak{C}}$ with $\varphi_{\vec{e}} \in (0, \pi)$ and $\theta_e \in (0, \pi)$. They parametrize circle patterns by (r_f) and (θ_e) (or (θ_e^*)), and call $(\varphi_{\vec{e}})$ a coherent angle system. One may consider deforming a circle pattern so as to have some θ_e approach 0 or π. The limit $\theta_e \to \pi$ is easy to picture, one simply gets that the two circles $C_f, C_{f'}$ of the adjacent faces become tangent. The limit $\theta_e \to 0$ is a bit more complex, as the final shape of Q_e (the quadrangle associated to e) may depend on $\varphi_{\vec{e}}$ or $\varphi_{\overleftarrow{e}}$. If we parametrize circle patterns by (r_f) and (θ_e) as in [2], the limiting shape would depend on the relationship between r_f and $r_{f'}$. As our main result depends on extending [2] result to such limits and beyond, we find it more convenient to describe extended circle patterns by (r_f) and $(\varphi_{\vec{e}})$.

We will mostly be working with extended circle patterns that "look normal", with all $\varphi_{\vec{e}}$ in the range $[0, \pi)$, so we do not dwell on the meaning of negative $\varphi_{\vec{e}}$'s. [1]

Definition 4.2. An extended circle pattern is said to be *face non-singular* if $\Phi_f = 2\pi$ for all faces f; it is said to be *vertex non-singular* if $\sum_{e\ni v} \theta_e = 2\pi$ for all vertices v. Finally it is said to be *non-singular* if it is both.

[1] Intuitively, one can visualize decreasing $\varphi_{\vec{e}}$ from ε to $-\varepsilon$ as moving the black vertices of the quadrangle Q_e past each other, thus flipping Q_e along its long axis and making it have negative area.

Definition 4.3. Let f be a non-singular face (i.e. $\Phi_f = 2\pi$), such that for all edges $\vec{e} \in \partial f$, $\varphi_{\vec{e}} \in [0, \pi)$. We say f is *thin* if exactly two edges of f have nonzero $\varphi_\bullet$; we say it is *thick* otherwise. We say it is *convex* if for all edges $\vec{e} \in \partial f$, we have $\varphi_{\vec{e}} \in [0, \pi/2)$.

Definition 4.4. Given an extended circle pattern $c \in \underline{\mathfrak{C}}$, an edge e is *short* if it has length 0, $l_e = 0$; it is *long* otherwise.

Definition 4.5. Given an extended circle pattern $c \in \underline{\mathfrak{C}}$, a *wide path* is a sequence of faces $f_0, f_1, \ldots, f_n$ such that f_i, f_{i+1} share a long edge. A *wide cycle* is a wide path with $f_0 = f_n$.

Lemma 4.6. *Let c be a face non-singular extended circular pattern such that $\varphi_{\vec{e}} \geq 0$ for all $\vec{e} \in \vec{E}$. Furthermore, suppose that there is no cycle of edges $e_0, e_1, \ldots, e_n = e_0$ such that e_i, e_{i+1} belong to the same face, and $\varphi_{\vec{e_i}} = \varphi_{\overleftarrow{e_i}} = \pi/2$. Then $\underline{\mathfrak{C}}$ is a manifold in a neighborhood of c.*

Proof. We need to show that the differentials $d(l_{\vec{e}} - l_{\overleftarrow{e}}) = 2\sin\varphi_{\vec{e}} dr_{f_{\vec{e}}} + 2r_{f_{\vec{e}}}\cos\varphi_{\vec{e}} d\varphi_{\vec{e}} - 2\sin\varphi_{\overleftarrow{e}} dr_{f_{\overleftarrow{e}}} - 2r_{f_{\overleftarrow{e}}}\cos\varphi_{\overleftarrow{e}} d\varphi_{\overleftarrow{e}}$ are linearly independent at c. If $\varphi_{\vec{e}} \neq \pi/2$, then the $d\varphi_{\vec{e}}$ term makes $d(l_{\vec{e}} - l_{\overleftarrow{e}})$ linearly independent from the rest (no other differential $d(l_{\vec{e'}} - l_{\overleftarrow{e'}})$ contains such component); likewise for $\varphi_{\overleftarrow{e}} \neq \pi/2$.

Now consider the set E' of edges e that have $\varphi_{\vec{e}} = \varphi_{\overleftarrow{e}} = \pi/2$. Consider a maximal sequence of faces $f_0, \ldots, f_n$ with no repetitions and f_i, f_{i+1} share an edge $e_i \in E'$. By the condition on no cycles, $f_0 \neq f_n$. By face non-singularity, any face can meet at most two edges from E', thus if $e \in E'$, it is contained in a unique such string of faces/edges. Thus the differentials $d(l_{\vec{e_i}} - l_{\overleftarrow{e_i}}) = 2dr_{f_i} - 2dr_{f_{i+1}}$ are linearly independent. □

4.1. **From Extended Circle Patterns to Hyperbolic Polyhedra.** In this section, we describe how to obtain a decomposition of a torihedron into hyperbolic ideal pyramids from a non-singular extended circle pattern.

Lemma 4.7. *Let $\mathcal{T}$ be a torihedron, with graph $\Gamma = \Gamma(\mathcal{T})$. Given a non-singular extended circle pattern $c \in \underline{\mathfrak{C}}$ on Γ, such that all $\varphi_{\vec{e}} \in (0, \pi)$, there exists a decomposition of $\mathcal{T}$ into base-angled ideal pyramids such that*

- *each interior edge of the torihedron has dihedral angles sum to 2π;*
- *each boundary edge e of the torihedron has dihedral angles sum to $\pi - \theta_e$.*

Proof. For each directed edge $\vec{e} \in \vec{E}$, construct the isosceles triangle $T_{\vec{e}}$ with equal sides of length $r_{f_{\vec{e}}}$ and angle $2\tilde{\varphi}_{\vec{e}}$ subtended between them, where $\tilde{\varphi}_{\vec{e}} = \varphi_{\vec{e}}$ if $\varphi_{\vec{e}}$ if it is acute, and $= \pi - \varphi_{\vec{e}}$ otherwise.

Let $f \in F$ be a face. We construct a Euclidean polygon Pol_f as follows. If $\varphi_{\vec{e}} \leq \pi/2$ for all $\vec{e} \in \partial f$, i.e. if f is convex, then the $T_{\vec{e}}$ for $\vec{e} \in \partial f$ fit together into Pol_f. If not, suppose $\varphi_{\vec{e}} > \pi/2$ for $\vec{e} = \vec{e_1}$, and $\leq \pi/2$ for $\vec{e} = \vec{e_2}, \ldots \vec{e_k} \in \partial f$. Then put $T_{\vec{e_2}}, \ldots, T_{\vec{e_k}}$ together as above, creating a $(k+1)$-gon, then subtract $T_{\vec{e_1}}$ from it to form Pol_f.

Thus, to each face, we associate the Euclidean polygon Pol_f. If v is the vertex of Pol_f between e_i and e_{i+1}, then the angle at v is $\pi - \varphi_{\vec{e_i}} - \varphi_{\vec{e_{i+1}}}$. Then the non-vertex-singularity of c guarantees that the sum of angles at v of Pol_f, for faces f containing v, is 2π.

View the Euclidean plane as the boundary of the upper-half space. Then Pol_f supports an ideal hyperbolic pyramid P_f.

Clearly, these P_f's, as abstract ideal tetrahedra, glue together into the torihedron. We need to check that the angles around each edge of the torihedron have the appropriate angles.

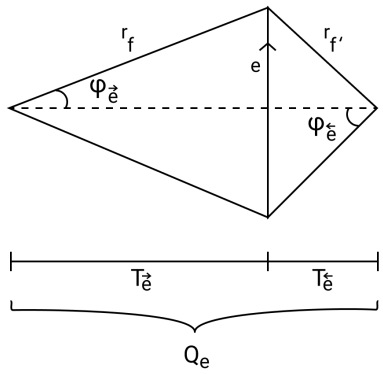

FIGURE 16. The quadrangle associated to the edge e between two convex faces.

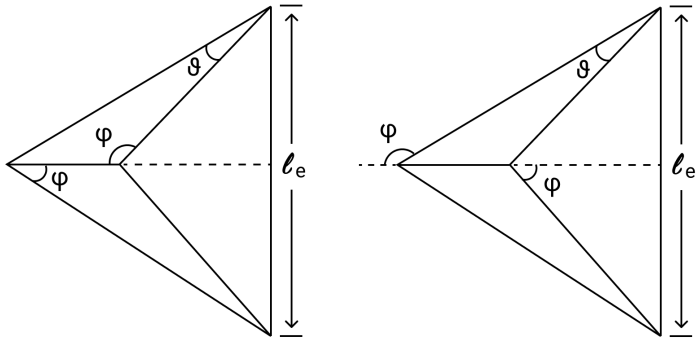

FIGURE 17. Left: Quadrangle when θ_e is small and positive; Right: Quadrangle when θ_e is small and negative, so it takes up "negative area" (see proof of Lemma 4.7).

Consider an interior edge e of the pyramidal decomposition of the torihedron. It corresponds to a vertex v of the graph. Note that the dihedral angle of the vertical edge at v of P_f is simply the angle at v of Pol_f; these sum to 2π over $f \ni v$.

For a boundary edge e, the dihedral angles at e of the P_f's containing it are $\varphi_{\vec{e}}$ and $\varphi_{\overleftarrow{e}}$, which sum to θ_e by definition.

□

4.2. **Deforming Extended Circle Patterns.** Our general strategy for obtaining a (non-singular) circle pattern is to start with an assignment $\underline{\theta} = (\theta_\bullet)$ for which we know an extended circle pattern exists (say from results of [2]), and a path γ in $\underline{\mathbf{\Theta}}$ starting at $\underline{\theta}$. We then attempt to lift γ to a path $\tilde{\gamma}$ in $\underline{\mathfrak{C}}$, so that $\tilde{\gamma}$ remains (face) non-singular (vertex non-singularity is already determined by γ).

Note that since $\sum_{e\in E}\theta_e = 2\pi|E| - \sum_{\vec{e}\in\vec{E}}\varphi_{\vec{e}} = 2\pi|E| - \sum_{f\in F}\Phi_f$, we see that maintaining face non-singularity of $\tilde{\gamma}$ forces $\sum\theta_e$ to be constant. We will show that this is the only obstruction on γ to the lifting to such $\tilde{\gamma}$.

To that end, let L be the $(|E|-1)$-plane distribution on $\underline{\mathbf{\Theta}}$ tangent to the level sets of $\sum_{e\in E}\theta_e$. The following proposition proves that we can deform some circle patterns up to first order at a point:

Proposition 4.8. *Let $c \in \underline{\mathfrak{C}}$ be a non-singular extended circle pattern on a graph with no bigons or self-loops such that there is no wide cycle of thin faces, and each edge meets two distinct faces. Let $K_c = \ker(\Phi_*|_c : T_c\underline{\mathfrak{C}} \to T_{\Phi(c)}\underline{\mathbf{\Phi}})$. Then $\Theta_*(K_c) = L_{\Theta(c)}$.*

In other words, for any vector $a \in T_{\Theta(c)}\underline{\mathbf{\Theta}}$ with sum of components 0, one can vary c so that its first order change in $\theta_\bullet$ is a, and also remains face non-singular up to first order.

Before we prove this, it is convenient to first prove the following, which will establish some useful notation:

Lemma 4.9. *Let $c \in \underline{\mathfrak{C}}$ be as in Proposition 4.8. Then Φ is a submersion in a neighborhood of c.*

Proof. We construct vectors $\beta_f \in T_c\underline{\mathfrak{C}}$ so that $\Phi_*(\beta_f) = \frac{\partial}{\partial\Phi_f}$. The vector

$$\alpha_f := \frac{\partial}{\partial r_f} - \sum_{\vec{e}\in\partial f} \frac{\tan\varphi_{\vec{e}}}{r_f}\frac{\partial}{\partial\varphi_{\vec{e}}} \in T(\underline{\mathfrak{R}}\times\underline{\mathfrak{Q}}) \tag{1}$$

doesn't change $l_{\vec{e}}$, so is in $T_c\underline{\mathfrak{C}}$. Intuitively, α_f is like pulling the center of C_f up off the plane, increasing r_f and decreasing all φ's. Its pushforward under Φ is simply $\Phi_*(\alpha_f) = (-\frac{2}{r_f}\sum_{\vec{e}\in\partial f}\tan\varphi_{\vec{e}})\frac{\partial}{\partial\Phi_f}$.

If f is a convex face, then the $\tan\varphi_{\vec{e}}$ are all non-negative, being 0 if and only if e is short, and because $\Phi_f = 2\pi$, at least three edges are long. So $\Phi_*(\alpha_f)$ is a negative multiple of $\frac{\partial}{\partial\Phi_f}$; we choose β so that

$$\beta_f := \beta\cdot\alpha_f; \quad \Phi_*(\beta_f) = \frac{\partial}{\partial\Phi_f} \tag{2}$$

If f is thick but not convex, let $\vec{e}$ be an edge with largest $\varphi_{\vec{e}}$, so that $\varphi_{\vec{e}} \geq \pi/2$. If $\varphi_{\vec{e}} > \pi/2$, then since tan is convex, and f has at least two other long edges, we see that $\Phi_*(\alpha_f) = -\sum\frac{\tan\varphi_{\vec{e}'}}{r_f} > 0$, so we can define β_f as in (2). If $\varphi_{\vec{e}} = \pi/2$, we can take

$$\beta_f = \frac{1}{2}\frac{\partial}{\partial\varphi_{\vec{e}}}$$

If f is thin, we actually have that $\alpha_f \in K_c$, since the components sum to 0, so we need a different approach. First suppose f shares an edge e with a thick face f', with $\vec{e}\in\partial f$. If $\varphi_{\vec{e}} = \pi/2$, we can take $\beta_f = \frac{1}{2}\frac{\partial}{\partial\varphi_{\vec{e}}}$ as before. Otherwise, we can increase $l_{\vec{e}}$ by varying $\varphi_{\vec{e}}$ while holding r_f constant, and increase $l_{\overleftarrow{e}}$ by increasing $r_{f'}$. This will affect both $\Phi_f, \Phi_{f'}$, so we use $\beta_{f'}$ to make $\Phi_{f'}$ constant. We can repeat this procedure with f' set to this thin face, and f set to another thin face adjacent to it, etc. □

Proof. We construct a vector $u_e \in K_c \subseteq T_c\underline{\mathfrak{C}}$ for each edge e and show that $\{\Theta_*(u_e)\}_{e\in E}$ spans an $|E|-1$ dimensional space, thus must be equal L_{Θ_c}. The vectors u_e will have the following property: if $\Theta_*(u_e) = \sum_{e'\in E} a^{e'}\frac{\partial}{\partial\theta_{e'}}$, then

- $a^e = 1$;
- $a^{e'} \leq 0$ for all $e' \neq e$;
- $\sum_{e'\in E} a^{e'} = 0$ (follows directly from $u_e \in K_c$)

Furthermore, these u_e's collectively satisfy the following connectivity property: consider the graph G whose vertex set is the set of edges E, and we connect two long edges e, e' by an edge if there is some e'' such that $a^e, a^{e'}$ are both nonzero in $\Theta_*(u_{e''})$; then G is connected.

Let us first suppose we have constructed such u_e, and show that these properties ensure that $\{\Theta_*(u_e)\}_{e\in E}$ spans an $|E|-1$ dimensional space. This is a simple exercise in linear algebra, but we show it for completeness.

Put the $\Theta_*(u_e)$'s into a $E \times E$ matrix, denoted M, so that the e-th row corresponds to $\Theta_*(u_e)$. By virtue of $u_e \in K_c$, we have that $(1\ 1\ \cdots\ 1)^T$ is in the null space of M; our goal is to show that it spans the null space.

Suppose $b = (b_e)^T$ is in the null space of M. Let $|b_e|$ be the largest among components of b; rescale b so that $b_e = 1$. The e-th component of Mb is $1 - \sum_{e'\neq e} a^{e'} b_{e'}$, where $a^{e'}$ are the components of $\Theta_*(u_e)$. Since $\sum_{e'\neq e} |a^{e'}| = 1$, this can be 0 if and only if for all e' with $a^{e'} < 0$, we have exactly $b_{e'} = 1$. We then repeat this argument on the other e' that appear in $\Theta_*(u_e)$. By connectedness of G, this implies $b = (1\ \cdots\ 1)^T$, thus M has rank $|E|-1$.

Before constructing the u_e's, let us first construct several other auxiliary vectors that are not in $T_c\underline{\mathfrak{C}}$. Generally they keep Φ_f's constant, but have an effect on the lengths of oriented edges $l_{\vec{e}}$. The u_e's will be built from a combination of these. All discussion of changes will refer to changes in the first order.

Let f be a convex face, and $\vec{e} \in \partial f$. Define

$$\eta_{\vec{e}} = \frac{1}{2r_f \cos\varphi_{\vec{e}}} \frac{\partial}{\partial \varphi_{\vec{e}}} - \frac{1}{r_f \cos\varphi_{\vec{e}}} \beta_f \tag{3}$$

$\eta_{\vec{e}}$ keeps Φ_f constant, but increases $l_{\vec{e}}$ at unit speed, i.e. $dl_{\vec{e}}(\eta_{\vec{e}}) = 1$.

Let f be a thick but not convex face. There is exactly one edge $\vec{e} \in \partial f$ with $\varphi_{\vec{e}} \geq \pi/2$. If $\varphi_{\vec{e}} > \pi/2$, we will define $\eta_{\vec{e}}$ as in (3). If $\varphi_{\vec{e}} = \pi/2$, we will define

$$\eta_{\vec{e}} = \frac{1}{2}\frac{\partial}{\partial r_f} + \Big(\sum_{\vec{e'}\neq\vec{e}} \frac{\sin\varphi_{\vec{e'}}}{2r_f\cos\varphi_{\vec{e'}}}\Big)\frac{\partial}{\partial\varphi_{\vec{e}}} - \sum_{\vec{e'}\neq\vec{e}} \frac{\sin\varphi_{\vec{e'}}}{2r_f\cos\varphi_{\vec{e'}}}\frac{\partial}{\partial\varphi_{\vec{e'}}} \tag{4}$$

Then it is easy to see that $dl_{\vec{e}}(\eta_{\vec{e}}) = 1$ while $dl_{\vec{e'}}(\eta_{\vec{e}}) = 0$ for all other $\vec{e'} \neq \vec{e}$, and $\eta_{\vec{e}}$ keeps Φ_f constant.

Now let $\vec{e'} \in \partial f$ be another edge. We define

$$\gamma_{\vec{e'}} = \frac{1}{2r_f\cos\varphi_{\vec{e'}}}\Big(\frac{\partial}{\partial\varphi_{\vec{e'}}} - \frac{\partial}{\partial\varphi_{\vec{e}}}\Big) \tag{5}$$

Then $dl_{\vec{e'}} = 1$, $dl_{\vec{e}} = -\frac{\cos\varphi_{\vec{e}}}{\cos\varphi_{\vec{e'}}} \geq 0$, and keeps Φ_f constant.

Finally, let f be a thin face. If $\vec{e} \in \partial f$ is a short edge, i.e. $\varphi_{\vec{e}} = 0$, then we define $\eta_{\vec{e}}$ as in (3). If $\vec{e}$ is long, and $\varphi_{\vec{e}} \neq \pi/2$, we define $\gamma_{\vec{e}}$ as in (5); if $\varphi_{\vec{e}} = \pi/2$, we define

$$\xi_{\vec{e}} = \frac{1}{2}\frac{\partial}{\partial r_f} \tag{6}$$

Clearly $dl_{\vec{e}}(\xi_{\vec{e}}) = dl_{\vec{e'}}(\xi_{\vec{e}}) = 1$ for the other edge e' with $\varphi_{\vec{e'}} = \pi/2$.

In summary, $\eta_{\vec{e}}, \gamma_{\vec{e}}, \xi_{\vec{e}}$ always increases $l_{\vec{e}}$ at unit speed, and keeps $\Phi_{f_{\vec{e}}}$ constant. $\eta_{\vec{e}}$ does not affect the lenghts of other edges in the face $f_{\vec{e}}$, but the other two might affect another edge - this other edge $\vec{e'}$ is unique, and $l_{\vec{e}}, l_{\vec{e'}}$ either both increase or decrease. Furthermore, $l_{\vec{e'}} \geq l_{\vec{e}}$.

For any oriented edge $\vec{e}$, there is exactly one such vector defined for it; call that vector $\zeta_{\vec{e}}$.

Now we can put these vectors together to construct the desired u_e's. To illustrate the main idea of the construction, first suppose that e is an edge between two convex faces f, f'. Then we can consider

$$w_e = \eta_{\vec{e}} + \eta_{\overleftarrow{e}}$$

Since $dl_{\vec{e}}(w_e) = dl_{\overleftarrow{e}}(w_e) = 1$, and $dl_{\vec{e'}}(w_e) = 0$ for all other edges, $w_e \in T_c\underline{\mathfrak{C}}$; furthermore, η_- does not affect Φ_-, so $w_e \in K_c$. For $\vec{e'} \in \partial f \cup \partial f' \backslash \{\vec{e}, \overleftarrow{e}\}$, the $\frac{\partial}{\partial \varphi_{\vec{e'}}}$ component only appears in β_f or $\beta_{f'}$, which is positive by construciton (because f, f' are convex faces); thus, $d\theta_{e'}(w_e) \geq 0$ for such e', and is equal to 0 if and only if e' is short. Finally, since $w_e \in K_c$, it leaves the sum $\sum_{e \in E} \theta_e$ constant, so $d\theta_e(w_e) < 0$, so we can take

$$u_e := (d\theta_e(w_e))^{-1} \cdot w_e \tag{7}$$

Now consider an arbitrary edge e between faces f, f'. We build u_e inductively, beginning with $w_e = \zeta_{\vec{e}} + \zeta_{\overleftarrow{e}}$, $F' = \{f, f'\}$, and $E' = \{e\}$. If w_e also affects $l_{\vec{e'}}$ for some edge $\vec{e'} \in \partial F' \backslash \{\vec{e''}, \overleftarrow{e''} | e'' \in E'\}$, we add an appriopriate positive multiple of $\zeta_{\overleftarrow{e'}}$ to w_e, add $f_{\overleftarrow{e'}}$ to F', and add e' to E'. Recall that when $\zeta_{\vec{e'}}$ affects the length of another edge e'', we always have $l_{\vec{e''}} \geq l_{\vec{e'}}$. Thus by the condition of non-existence of wide cycles of thin faces, this process must terminate. It is not hard to see that when an η_- term appears, the process terminates (for that direction); a γ_- term begets either another γ_- or η_- term; a ξ_- term begets either a ξ_-, γ_-, or η_- term. In other words, in the end we get some sum (ignoring possible positive coefficients)

$$w_e = (\xi_- + \xi_- + \cdots + \gamma_- + \gamma_- + \cdots + \eta_-) + (\xi_- + \xi_- + \cdots + \gamma_- + \gamma_- + \cdots + \eta_-)$$

where in each parenthesis, the first term affects the next term and so on.

Assume that there are no thin faces. We check that w_e has the desired properties. By construction, $w_e \in T_c\underline{\mathfrak{C}}$. Observe that the coefficient of $\frac{\partial}{\partial \varphi_{\vec{e}}}$ is positive in either $\eta_{\vec{e}}$ or $\gamma_{\vec{e}}$, so $d\theta_e(\Theta_*(w_e)) < 0$. There is a maximal sequence of thick faces $f_0 = f, f_1, \ldots, f_n$ and a sequence of edges $e_0 = e, e_1, \ldots, e_n$, where for $i \neq 0$, e_i is between f_{i-1} and f_i, and l_{e_i} increases under w_e; we label oriented edges so $\vec{e_i} \in \partial f_i$, $\overleftarrow{e_i} \in \partial f_{i+1}$. (Similar discussion for $f_0 = f'$). Consider one of the edges e_i, $i \neq 0$. Since l_{e_i} increases, the $\zeta_{\vec{e}_{i-1}}$ term from the previous edge e_{i-1} must have been $\gamma_{\vec{e}_{i-1}}$; in particular, $\varphi_{\overleftarrow{e_i}} > \pi/2$, w_e decreases $\varphi_{\overleftarrow{e_i}}$, and keeps $r_{f_{i-1}}$ constant. The edge e_i also contributes some $\zeta_{\vec{e_i}}$ term to w_e; it increases $\varphi_{\vec{e_i}}$ and either increases or keeps constant r_{f_i}. Then θ_{e_i} increases, i.e. $d\theta_{e_i}(\Theta_*(w_e)) > 0$, by the following simple exercise in elementary Euclidean geometry. Suppose we have an obtuse triangle $\triangle ABC$, $\angle B > \pi/2$, and we decrease $\angle B$, increase $\angle C$, keep length of $\overline{AB}$ constant, and either increase or keeps constant the length of $\overline{AC}$; then $\angle A$ increases. This can be proved by observing that the changes we are forcing on the triangle can be broken in two: the first is increase $\angle B$ and keeping lengths $\overline{AB}, \overline{AC}$ constant, and the second is keeping $\angle B$ and length $\overline{AB}$ constant, and increasing length $\overline{AC}$; each of these steps increases $\angle A$. We apply this to our situation with B, C being the centers of circles $C_{f_{i-1}}, C_{f_i}$ of the faces f_{i-1}, f_i. As before, we simply rescale w_e appropriately to obtain u_e.

Now we consider the presence of thin faces. If all the ζ_- terms added to w_e are η_- or γ_-, then all arguments in the previous paragraph applies. The only situation in which ξ_- is used is when either $\zeta_{\vec{e}}$ or $\zeta_{\overleftarrow{e}}$ is ξ_-. Without loss of generality, $\zeta_{\vec{e}} = \xi_{\vec{e}}$, so that $\vec{e} \in \partial f$, f is a thin face with nonzero angles equal to $\pi/2$; let $\vec{e'}$ be the other edge with φ angle $\pi/2$. Suppose the next face, the one adjacent to e', is not thin. We simply add $\alpha \cdot (\frac{\partial}{\partial \vec{e}} - \frac{\partial}{\partial \vec{e'}})$ to

w_e, where $\alpha > 0$ is chosen small enough so that, in combination with the next w_e term $\zeta_{e'}^{\leftarrow}$, $\theta_{e'}$ increases; for example, if the next term is $\zeta_{e'}^{\leftarrow} = \gamma_{e'}^{\leftarrow}$, then we choose $\alpha < \frac{1}{2r\cos\varphi_{e'}^{\leftarrow}}$, the coefficient of $\frac{\partial}{\partial\varphi_{e'}^{\leftarrow}}$ in $\gamma_{e'}^{\leftarrow}$. If the next face is also thin, we add the same term, and so on, until we reach a non-thin face. It is straighforward to check that θ_e decreases, and all other affected θ_-'s increase. □

Proposition 4.10. *Let $c \in \underline{\mathfrak{C}}$ be as in Proposition 4.8. Given a smooth path $\gamma : [0,\infty) \to \underline{\mathbf{\Theta}}$ starting at $\gamma(0) = \Theta(c)$ and has constant value $(\sum\theta_e)\circ\gamma$, there exists $\varepsilon > 0$ and a lift $\tilde{\gamma} : [0,\varepsilon] \to \underline{\mathfrak{C}}$ of $\gamma|_{[0,\varepsilon]}$ along Θ that starts at $\tilde{\gamma}(0) = c$ and has constant value $\Phi\circ\tilde{\gamma}$.*

Proof. By Lemma 4.9, Φ is a submersion at c, hence is a submersion in a neighborhood $U \in \underline{\mathfrak{C}}$ of c. Thus, the kernels $K_{c'} = \ker(\Phi_*|c' : T_{c'}\underline{\mathfrak{C}} \to T_{\Phi(c')}\underline{\mathbf{\Phi}})$ form an $|E|$-plane distribution $K \subset T\underline{\mathfrak{C}}|_U$ over U. By Proposition 4.8, the bundle map $\Theta_*|_K : K \to L$ is full rank at c, hence it is full in a possibly smaller neighborhood, which we redefine U to be.

Since $\sum_{e\in E}\theta_e = 2\pi|E| - \sum_{f\in F}\Phi_f$, the fullness of Φ_* also shows that $\sum\theta$ has no critical points in U; for s in some small interval around $(\sum\theta)(c)$, denote, by overloading notation, $L_s = (\sum\theta)^{-1}(s)$, $U_s = U \cap \Theta^{-1}(L_s)$. We may consider K as a family of $|E|$-plane distributions K_s over U_s.

The vector $\rho := \sum_{f\in F} r_f\frac{\partial}{\partial r_f}$ corresponds to scaling all radii by the same factor, and is clearly in $T\underline{\mathfrak{C}}$. It is obviously mapped to zero under Φ_* and Θ_*, so $\operatorname{span}\{\rho\} = \ker(\Theta_*|_K) \subset K$. Thus, over U, we may split $K = \operatorname{span}\{\rho\} \oplus K'$ (say as orthogonal decomposition w.r.t. some smooth metric on $\underline{\mathfrak{C}}$), so that $\Theta_*|c' : K'|_{c'} \simeq L_{\Theta(c')}$.

In other words, $K'|_{U_s}$ is a horizontal $(|E|-1)$-plane distribution that determines an Ehresmann connection of the fibre bundle $U_s \to L_s$ (after being appropriately restricted). Therefore, a short path γ starting at $\Theta(c)$ with constant $\sum\theta$, i.e. a path in L_s, $s = (\sum\theta)(c)$, can be lifted to a path $\tilde{\gamma}$ in U_s, so that $\tilde{\gamma}$ is always tangent to K', hence $\Phi(\tilde{\gamma})$ is constant. □

Finally let us say a few words in relation to the proof of hyperbolicity of augmented links, i.e. the proof of Theorem 3.6. Using Theorem 4 from [2], we obtain an angle-splitting for the $\pi/2$-angled torihedra in the torihedral decomposition of the original link K. This allows us to get a "degenerate" circle pattern for $\Gamma_T(L)$: an edge with label $\theta_e^* = \pi$ separates a triangular face t from a bowtie with a face f which corresponds to a face in the original graph $\Gamma_T(K)$; we will take the circumcircle of t to be the same as that of f; an edge with $\theta_e^* = 0$ then separates two circles that are tangent. Now we apply Proposition 4.10, possibly adding some edges and using the $+$'s and $-$'s as in Figure 14, to obtain an extended circle pattern on $\Gamma_T(L)$ that has all $\theta^* > 0$. By Lemma 4.7, we obtain a decompositiion of the torihedron $\mathcal{T}_T$ into ideal hyperbolic pyramids. We do the same for the bottom torihedron $\mathcal{T}_B$. Finally, as before, we can cut up these hyperbolic ideal pyramids into ideal tetrahedra, thus obtaining a hyperbolic triangulation of the link complement $\mathbb{T}^2 \times I - L$.

Remark 4.11. It is not clear to us how to extend the proof of Theorem 3 [2] to allow $\theta \geq \pi$, as we no longer have convexity of S_{Euc}.

References

[1] Colin C. Adams. Augmented alternating link complements are hyperbolic. In *Low-dimensional topology and Kleinian groups (Coventry/Durham, 1984)*, volume 112 of *London Math. Soc. Lecture Note Ser.*, pages 115–130. Cambridge Univ. Press, Cambridge, 1986.

[2] Alexander I. Bobenko and Boris A. Springborn. Variational principles for circle patterns and Koebe's theorem. *Trans. Amer. Math. Soc.*, 356(2):659–689, 2004.

[3] Abhijit Champanerkar, Ilya Kofman, and Jessica S. Purcell. Geometry of biperiodic alternating links. *J. Lond. Math. Soc. (2)*, 99(3):807–830, 2019.

[4] L. R. Ford, Jr. and D. R. Fulkerson. *Flows in networks*. Princeton Landmarks in Mathematics. Princeton University Press, Princeton, NJ, 2010. Paperback edition [of MR0159700], With a new foreword by Robert G. Bland and James B. Orlin.

[5] David Futer and François Guéritaud. From angled triangulations to hyperbolic structures. In *Interactions between hyperbolic geometry, quantum topology and number theory*, volume 541 of *Contemp. Math.*, pages 159–182. Amer. Math. Soc., Providence, RI, 2011.

[6] Marc Lackenby. The volume of hyperbolic alternating link complements. *Proc. London Math. Soc. (3)*, 88(1):204–224, 2004. With an appendix by Ian Agol and Dylan Thurston.

[7] William W. Menasco. Polyhedra representation of link complements. In *Low-dimensional topology (San Francisco, Calif., 1981)*, volume 20 of *Contemp. Math.*, pages 305–325. Amer. Math. Soc., Providence, RI, 1983.

[8] W. P. Thurston. The geometry and topology of three-manifolds. Princeton Univ. Math. Dept. Notes. Available at http://www.msri.org/communications/books/gt3m. [2, 21, 50, 58, 68, 87, 89, 94, 97, 99, 138, 196], 1979.